NANO LETTERS

Letter

pubs.acs.org/NanoLett

Distance Dependence of the Energy Transfer Rate from a Single Semiconductor Nanostructure to Graphene

François Federspiel,[†] Guillaume Froehlicher,[†] Michel Nasilowski,[‡] Silvia Pedetti,[‡] Ather Mahmood,[†] Bernard Doudin,[†] Serin Park,[§] Jeong-O Lee,[§] David Halley,[†] Benoît Dubertret,[‡] Pierre Gilliot,[†] and Stéphane Berciaud*[,†]

[†]Institut de Physique et Chimie des Matériaux de Strasbourg and NIE, UMR 7504, Université de Strasbourg and CNRS, 23 rue du Lœss, BP43, 67034 Strasbourg Cedex 2, France

[‡]Laboratoire de Physique et d'Etude des Matériaux, ESPCI-ParisTech, PSL Research University, Sorbonne Université UPMC Univ Paris 06, CNRS, 10 rue Vauquelin 75005 Paris, France

[§]Advanced Materials Division, Korea Research Institute of Chemical Technology, Daejeon 305-343, Korea

S *Supporting Information*

ABSTRACT: The near-field Coulomb interaction between a nanoemitter and a graphene monolayer results in strong Förster-type resonant energy transfer and subsequent fluorescence quenching. Here, we investigate the distance dependence of the energy transfer rate from individual, (i) zero-dimensional CdSe/CdS nanocrystals and (ii) two-dimensional CdSe/CdS/ZnS nanoplatelets to a graphene monolayer. For increasing distances d, the energy transfer rate from individual nanocrystals to graphene decays as $1/d^4$. In contrast, the distance dependence of the energy transfer rate from a two-dimensional nanoplatelet to graphene deviates from a simple power law but is well described by a theoretical model, which considers a thermal distribution of free excitons in a two-dimensional quantum well. Our results show that accurate distance measurements can be performed at the single particle level using graphene-based molecular rulers and that energy transfer allows probing dimensionality effects at the nanoscale.

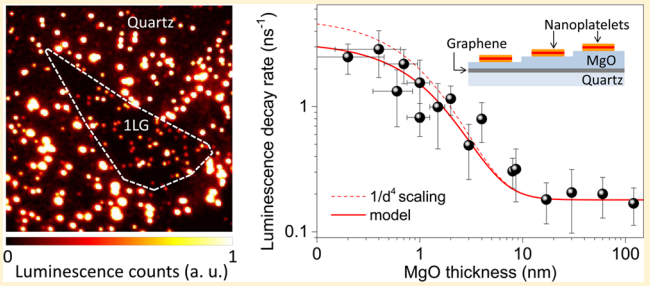

KEYWORDS: *Graphene, semiconductor nanocrystals, quantum dots, semiconductor nanoplatelets, quantum wells, resonant energy transfer, FRET, single molecule luminescence, heterostructures, dimensionality*

Graphene and colloidal semiconductor nanostructures are model low-dimensional systems, which hold promise for optoelectronic applications.[1−3] On the one hand, graphene, as a quasi-transparent semimetal[4,5] with excellent transport properties,[6] can be seen as an ultimate transparent electrode.[7,8] On the other hand, colloidal semiconductor nanostructures, in the form of zero-dimensional nanocrystals[9] (NCs or quantum dots), one-dimensional quantum rods,[10] and two-dimensional nanoplatelets[11,12] (NPs, or quantum wells), are very efficient broadband light harvesting systems and size hypenize tunable nanoemitters, which are intensively used in a new generation of light-emitting diodes, solar cells, and photovoltaic devices.[3]

There is a growing interest in combining graphene and colloidal semiconductor nanostructures in the form of hybrid systems[13−15] and devices[16−19] with new functionalities and potentially enhanced optoelectronic properties. The photoresponse of the graphene NC−hybrid system is governed by interface and short-range phenomena, such as charge transfer and Förster-type resonant energy transfer[20] (RET) (see Figure 1). While photoinduced charge transfer may result in a photogating effect and improved photogain,[16,17] energy transfer from a photoexcited colloidal semiconductor nanostructure (donor) to a graphene layer (acceptor) may efficiently generate electron−hole pairs in graphene, which is of interest for optoelectronics.[2] Importantly, graphene stands out as a uniquely tunable acceptor system, in which distinct regimes of RET can be observed by varying its Fermi level.[21−24]

Highly efficient RET from individual CdSe/ZnS NCs to graphene, resulting in a quenching of the luminescence signal by more than 1 order of magnitude, has recently been reported.[13] Related effects have been observed using other types of semiconductor nanostructures,[14,15,25−27] fluorescent molecules[28−30] or NV centers.[31,32] The observation of robust and efficient RET to graphene has stimulated numerous applications in biosensing[33] and holds promise for distance sensing[34] and photodetection. The case of a single colloidal semiconductor nanostructure near a single layer of graphene is of particular interest, since it provides a well-defined and technologically relevant system, in which the sensitivity of the RET rate to the local environment and its distance dependence

Received: November 17, 2014
Revised: January 14, 2015
Published: January 21, 2015

DOI: 10.1021/nl5044192
Nano Lett. 2015, 15, 1252−1258

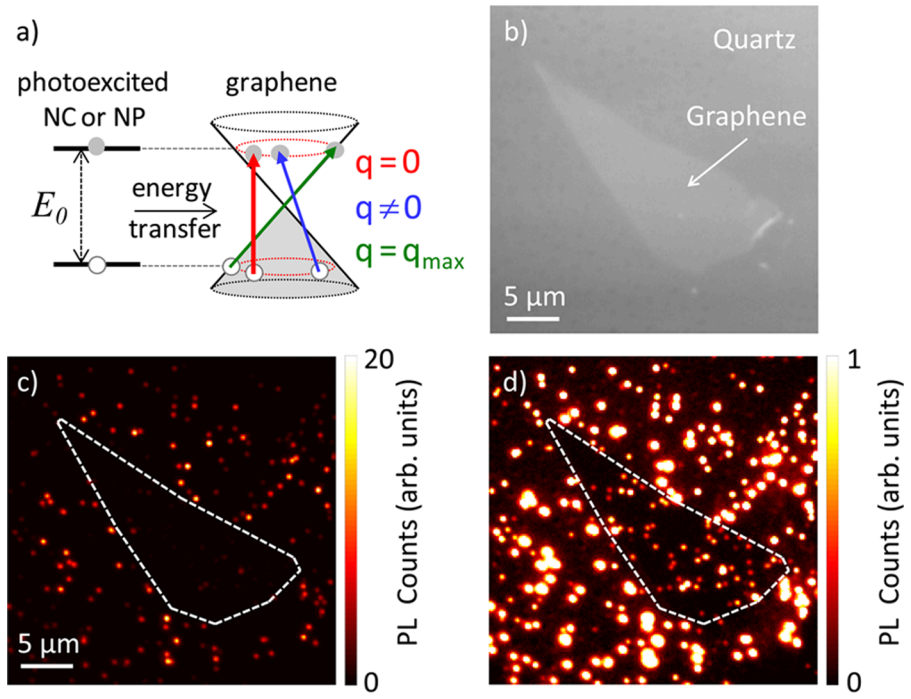

Figure 1. (a) Schematic representation of the resonant energy transfer process between a photoexcited nanoemitter and undoped graphene. Electronic excitations in graphene with various transferred momenta q are shown with colored arrows. (b) Optical image of an exfoliated graphene sample deposited on fused quartz. (c–d) Photoluminescence (PL) image of the same sample, covered with CdSe/CdS/ZnS nanoplatelets, shown with two different linear scales of PL intensity.

can be assessed with accuracy. In addition, RET is known to be strongly affected by exciton dimensionality and exciton localization.[35,36] Colloidal semiconductor nanostructures offer natural ways to explore such effects.

Here, we investigate RET from (i) individual core/shell CdSe/CdS NCs and (ii) core/shell CdSe/CdS/ZnS NPs to a graphene monolayer. Using molecular beam epitaxy, we are able to deposit ultrasmooth dielectric spacers of magnesium oxide (MgO), with variable thickness, between graphene and the nanoemitters.[37] The scaling of the RET rate with the distance d separating graphene from the nanoemitters is then quantitatively determined from the luminescence decays recorded on a collection of individual emitters. In the case of zero-dimensional NCs, the RET rate scales as $1/d^4$, as expected theoretically.[21,22,30,38−40] Interestingly, although the RET rate of individual two-dimensional NPs adsorbed on bare graphene is similar to that observed with zero-dimensional NCs, we find that the RET rate decays less rapidly with increasing distance. Such a behavior is discussed within the framework of energy transfer from free two-dimensional excitons[41,42] to a two-dimensional acceptor.

Methods. We have investigated individual colloidal semiconductor nanostructures near a graphene monolayer at room temperature, using a home-built microphotoluminescence (PL) setup equipped with a 100× (NA = 0.90) air objective. Core/shell CdSe/CdS NCs ((9.5 ± 1.5) nm in diameter, with a peak emission at λ_0 = 580 nm, i.e., photon energy of 2.14 eV), coated with oleylamine and oleic acid ligands, and core/shell/shell CdSe/CdS/ZnS NPs (4 monolayer thick core, ∼1.3 nm thick shell, ∼9 nm width, ∼22 nm length, and peak emission at λ_0 = 645 nm, i.e., photon energy of 1.92 eV), coated with oleate ligands, were synthesized following previous works[12,43−46] (see also Supporting Information). Using core/shell structures dramatically reduces the possibility of irreversible photoinduced NC or NP ionization and subsequent charge transfer to graphene.[46,47] NCs and NPs, dispersed at very low concentration into a 90%/10% hexane/octane mixture, were then dropcast onto graphene samples.

Measurements on bare graphene (see Figures 1−3) were performed using mechanically exfoliated graphene monolayers deposited on transparent fused quartz substrates. The distance dependence of the energy transfer rate was investigated using large area graphene monolayers, grown by low-pressure chemical vapor deposition (LPCVD) on a copper foil, then transferred onto a fused quartz substrate using standard methods[48] (see Supporting Information). In order to vary the distance between graphene and the nano emitters, thin films of MgO were grown on top of graphene in a staircase fashion in a molecular beam epitaxy (MBE) chamber[37] before deposition of NCs or NPs. We checked by atomic force microscopy that the roughness of the MgO layer is on the order of 0.5 nm.[49]

The bare graphene and graphene/MgO samples were characterized using a home-built micro-Raman setup (see Supporting Information). Although residual doping on the order of a few 10^{12} cm^{-2} could be observed, the resulting Fermi level shifts relative to the Dirac point are about 1 order of magnitude smaller than the energy of the emitted photons. Therefore, graphene will be considered as quasi-neutral in the following.

Individual NCs and NPs were excited using a pulsed supercontinuum laser, with a repetition rate tunable from 1.95 MHz up to 78 MHz. The unpolarized output of the supercontinuum laser at a wavelength of 480 nm (photon energy of 2.53 eV) was selected using an acousto-optic tunable filter. The full width at half-maximum of the filtered pulses was ≈50 ps. Wide-field PL images were recorded using an electron-multiplying charge coupled device camera (emCCD). PL time traces and PL decays of individual colloidal semiconductor

DOI: 10.1021/nl5044192
Nano Lett. 2015, 15, 1252−1258

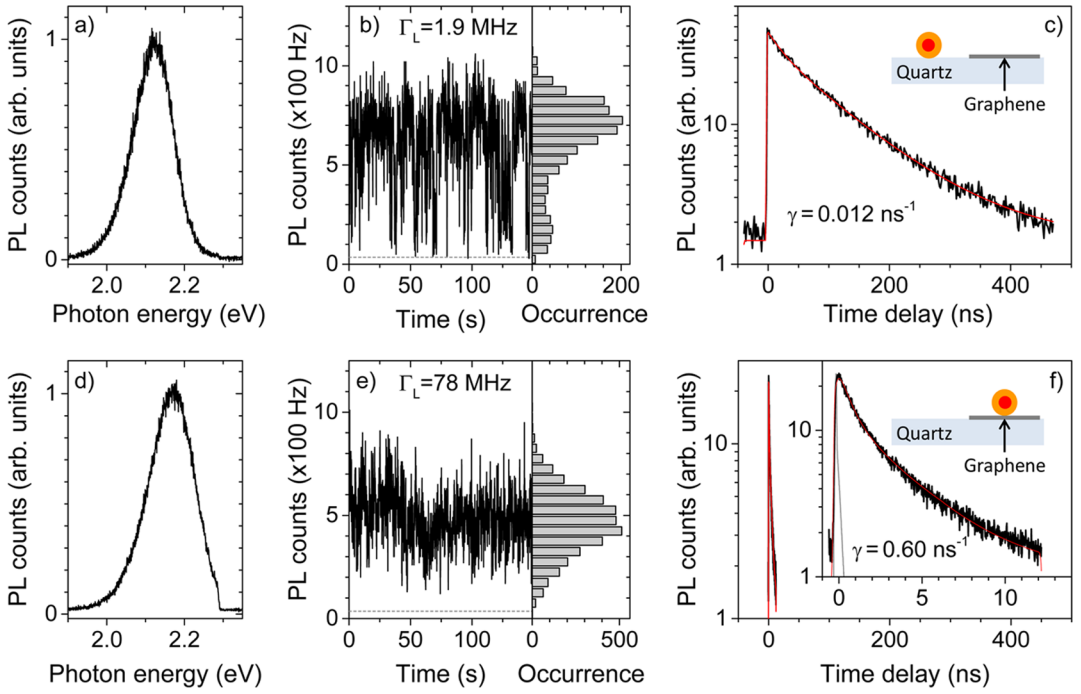

Figure 2. (a–c) Photoluminescence (PL) spectrum, PL time trace, and PL decay of individual CdSe/CdS nanocrystal deposited on fused quartz. (d–f) Same measurements recorded on an another individual CdSe/CdS nanocrystal deposited on a graphene monolayer. All data were collected using a pulsed laser excitation, with a repetition rate Γ_L indicated in panels b and e. The red lines in c and f are fits based on biexponential functions convoluted with the instrument response function (displayed as a gray line in f).

nanostructures were measured in a confocal arrangement, using an avalanche photodiode coupled to a time-tagged, time-correlated single photon counting board. PL spectra were recorded using a monochromator coupled to a CCD matrix. A pulse fluence lower than 1×10^{13} photons/pulse/cm^2 at λ = 480 nm was used for all measurements. Considering similar absorption cross sections of a few 10^{-14} cm^2 for our individual NCs and NPs at 480 nm,[50−52] we can estimate that on average, significantly less than one exciton per incoming laser pulse is formed in an individual NC or NP. We further verified that the PL decays of individual NCs and NPs are independent of the pulse fluence, in the range ($\approx 10^{12}$ to 3×10^{13} photons/pulse/cm^2).

Energy Transfer on Bare Graphene. Figure 1 shows wide-field PL images of individual CdSe/CdS/ZnS NPs deposited on a bare, mechanically exfoliated graphene monolayer. The PL intensity is strongly quenched, by more than 1 order of magnitude for NPs deposited on graphene. Very similar results were obtained using CdSe/CdS NCs. As previously discussed for individual core/shell CdSe/ZnS NCs,[13] we attribute PL quenching to Förster-type RET.

We then compare the typical PL spectrum, PL time trace, and PL decay of individual NCs (see Figure 2) and NPs (see Figure 3), measured on a fused quartz substrate and on a bare graphene monolayer. For each nanoemitter investigated, we introduce the average number of emitted photons per incoming laser pulse N_{em} (see PL time traces in Figures 2b,e and 3b,e). First, we note that, although the peak energy of the PL spectra exhibits a slight dispersion over a collection of nanoemitters, we did not observe systematic spectral shifts for NCs or NPs on graphene with respect to a reference on fused quartz. In both cases, the PL count rates on graphene and fused quartz are similar, but the PL signals are obtained using very different repetition rates (compare Figures 2b,e, and Figure 3b,e, for NCs and NPs, respectively). On these selected examples, N_{em} is quenched by a factor of approximately 50 (60) when the NC (NP) is adsorbed on graphene, as compared to a reference recorded on fused quartz. Over time scales larger than 100 ms, we also observe, in agreement with previous observations[13,14] that the blinking behavior, characteristic of NCs and NPs deposited on fused quartz, is seemingly reduced when the nanoemitters are adsorbed on graphene. This observation is presumably due to the acceleration of the excited state decay, which occurs before charge carriers may be trapped and allow the observation of dark and/or gray states.[46,53−56]

We now compare the PL decays of individual NCs and NPs measured on fused quartz and on graphene. Examples are shown in Figure 2c and f for individual NCs and in Figure 3c and f, for individual NPs, respectively. At this point, let us note that the room temperature typical PL decay of a single NC or NP is not monoexponential.[46,54−56] In the case of NCs, we found that most decays could be well fit to a biexponential form, while a stretched exponential form was providing better fits in the case of NPs. These complex behaviors are attributed to the existence of a distribution of bright, gray, and dark states with distinct lifetimes.[46,53−56] The fractional weight of these states in a measured decay may vary significantly from particle to particle, reflecting heterogeneities in core and shell passivation. In order to provide a general definition, the measured PL decay rate γ is defined as the maximum number of recorded counts divided by the (background corrected) total area of the PL decay. The resulting values are then multiplied by a correction factor, which takes into account the minor contribution of the instrument response function (see Figure 2c,f, Figure 3c,f, and Supporting Information). We have verified that our conclusions are independent of the method used to define the PL decay rate. For the individual NC (NP) considered here, we find that γ is enhanced by a factor of

DOI: 10.1021/nl5044192
Nano Lett. 2015, 15, 1252−1258

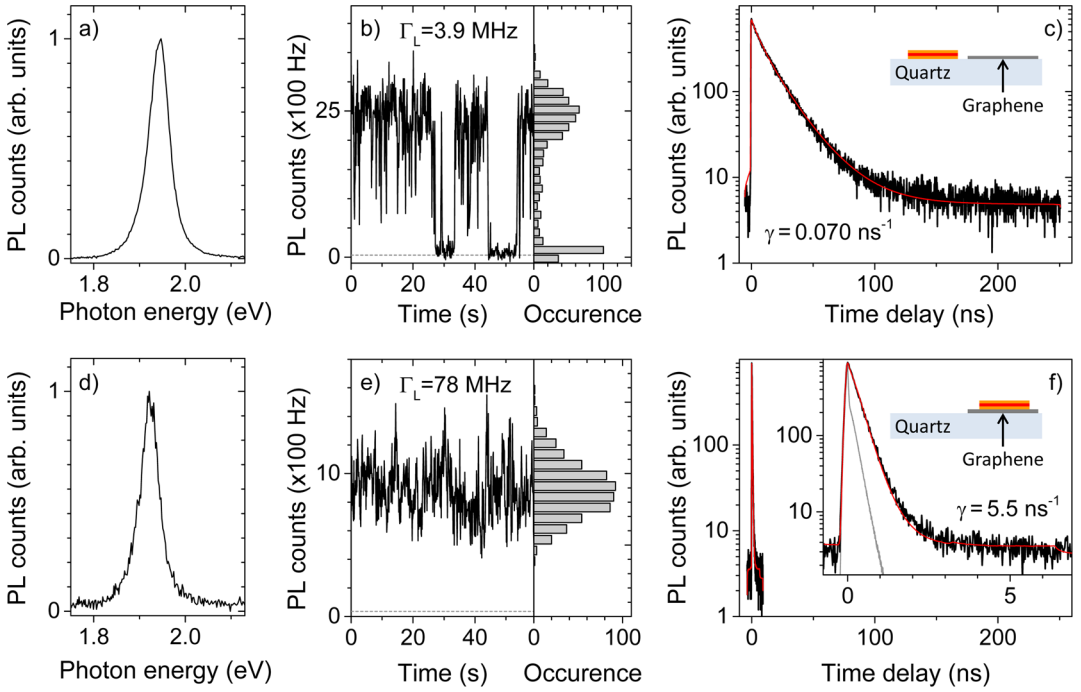

Figure 3. (a–c) Photoluminescence (PL) spectrum, PL time trace, and PL decay of an individual CdSe/CdS/ZnS nanoplatelet deposited on fused quartz. (d–f) Same measurements on another individual CdSe/CdS/ZnS nanoplatelet deposited on a graphene monolayer. All data were collected using a pulsed laser excitation, with a repetition rate Γ_L indicated in panels b and e. The red lines in c and f are fits based on stretched exponential functions convoluted with the instrument response function (displayed as a gray line in f).

approximately 50 (80). Remarkably, the quenching factors estimated from the PL time traces are in good agreement with the enhancement factors of the PL decay rate. This suggests that the strong PL quenching is solely due to an increase of the nonradiative decay rate and that possible modifications of the radiative decay rate of an individual NC or NP adsorbed on graphene can be neglected. This is consistent with recent theoretical calculations, which demonstrated that the radiative lifetime of an individual emitter is marginally modified in the vicinity of graphene.[22] Thus, in the following, we will consider that $\gamma \approx \gamma_t + \gamma_0$, where γ_t is the RET rate and γ_0 is the reference decay rate measured in the absence of graphene.

Similar measurements were repeated on more than 100 NCs and NPs deposited on bare graphene. We found similar statistically averaged quenching factors of approximately 50 for NCs and NPs. Overall, for 95% of the investigated single NCs and NPs, the RET efficiency, defined as $\eta = 1 - \gamma/\gamma_0$, is found to be larger than 95%.

Distance Dependence of the RET Rate. We have measured the PL decay of NCs and NPs separated from a graphene monolayer by a MgO thin film, with a thickness ranging from a few Å up to several tens of nanometers. In these experiments, the reference decay rate γ_0 is the statistically averaged decay rate of NCs and NPs measured on a bare >100 nm thick film of MgO. The results for NCs and NPs are summarized in Figures 4 and 5, respectively. Each point corresponds to a statistical average over 10 to 30 single NCs, and over more than 25 single NPs, respectively. The vertical error bars correspond to the standard deviations, while the horizontal error bars account for the roughness of the MgO film. For both NC and NPs, we observe that the measured decay rate decreases significantly, when increasing the thickness of the MgO film. However, as shown in Figures 4c and 5c, the product $N_{em}\gamma$ varies by less than a factor of 2 and, considering the standard deviations associated with each distribution, can be considered as constant. This generalizes the conclusions drawn from the analysis of Figures 2 and 3.

A key observation is that the decrease of the PL decay rate as a function of the MgO thickness is seemingly steeper for NCs than for NPs (see also Figure 7 in the Supporting Information for a comparison of the normalized decay rates). This points toward the effect of dimensionality on RET, which we now discuss. Let us first focus on the case of NCs interacting with graphene. Based on the well-known $1/d^6$ distance dependence of the Förster energy transfer rate between two point-like dipoles,[20] one would expect the measured decay rate to scale as

$$\gamma = \gamma_0 \left[1 + \left(\frac{z_0}{d_0 + d_{MgO}} \right)^p \right] \quad (1)$$

where the distance d separating the nanoemitter from the graphene layer is $d = d_0 + d_{MgO}$, with d_{MgO}, the thickness of the MgO film and d_0, the minimal distance between the center of the nanoemitter and the graphene surface in the absence of a MgO spacer, where z_0 characterizes the RET efficiency and p is related to the dimensionality of the donor and acceptor. A straightforward extension of Förster's theory would then give $p = 4$ for a zero-dimensional emitter interacting with a two-dimensional assembly of independent dipoles.[38,39] Indeed, for NCs (see Figure 4b, using $p = 4$, we obtain a good fit with $z_0 = (11.5 \pm 1.5)$ nm and $d_0 = (5.5 \pm 1)$ nm). The latter value is slightly larger than the average physical radius of the NCs, which is consistent with a possible contribution from the surrounding ligands and residual adsorbates to d_0.

Although a fit based on eq 1 is in good agreement with our measurements, one has to recall that eq 1 overlooks the fact that graphene is a two-dimensional system with extended, delocalized electronic wave functions and a well-defined

DOI: 10.1021/nl5044192
Nano Lett. 2015, 15, 1252–1258

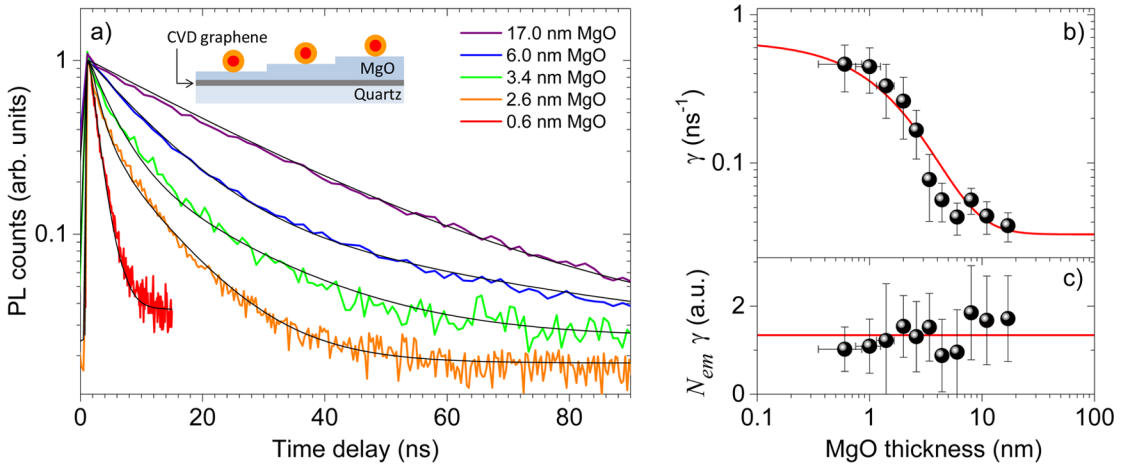

Figure 4. (a) Selected luminescence decays of individual CdSe/CdS nanocrystals separated from graphene by a MgO spacer graphene with increasing thicknesses. The thin black lines are fits based on biexponential decays convoluted with the instrument response function. (b) Statistically averaged measured decay rate γ as a function of the thicknesses of the MgO spacer. The red solid line is a fit based on eq 1, with $p = 4$, $d_0 = 5.5$ nm, $z_0 = 11.5$ nm. (c) Statistically averaged product of the number of emitted photons per exciting laser pulse N_{em} and the decay rate γ.

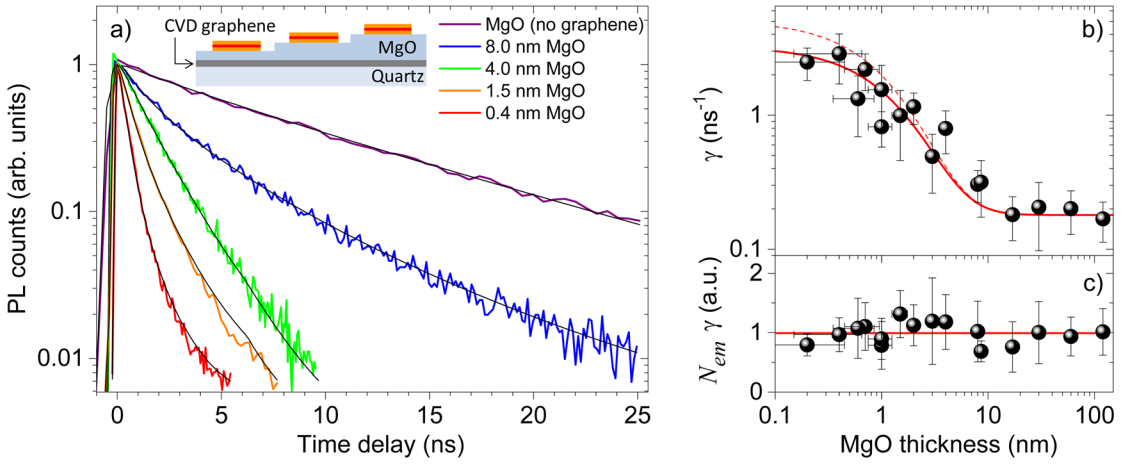

Figure 5. (a) Selected luminescence decays of individual CdSe/CdS/ZnS nanoplatelets separated from graphene by a MgO spacer graphene with increasing thicknesses. The thin black lines are fits based on stretched exponential decays convoluted with the instrument response function. (b) Statistically averaged measured decay rate γ as a function of the thicknesses of the MgO spacer. The red solid and dashed lines are fits based on eq 3, with $d_0 = 3.5$ nm, $\Lambda = 7.5$ nm, and on eq 1 with $p = 4$, $d_0 = 3.5$ nm, $z_0 = 8.0$ nm, respectively. (c) Statistically averaged product of the number of emitted photons per exciting laser pulse N_{em} and the decay rate γ.

electronic dispersion. The RET rate γ_t^{0D} from a single point-like dipole to graphene has been extensively studied theoretically in recent years[21,22,30,40,57,58] and can be written as[22,40]

$$\gamma_t^{0D} \propto \int_0^{q_{max}} \frac{dq\, q^3 e^{-2qd}}{\sqrt{q_{max}^2 - q^2}} \qquad (2)$$

where q is the transferred momentum, $q_{max} = 2\pi c/\lambda_0 v_F$ is the largest transferable momentum, λ_0 is the wavelength of the emitted photons, c is the speed of light, and $v_F \approx 1.1 \times 10^6$ m/s is the Fermi velocity in graphene. Contrary to far-field emission and absorption processes, the RET process described by eq 2 involves a finite momentum transfer (see Figure 1a), which is on the order of $1/d$. For neutral graphene, and distances such that $d \gg 1/q_{max} \approx 0.3$ nm, the denominator of the integrand in eq 2, which originates from the (momentum dependent) optical conductivity of graphene,[22] only gives significant contributions for $q \ll q_{max}$ (quasi-vertical transitions) and can thus be approximated as a constant. In these conditions, graphene can be treated as a two-dimensional assembly of incoherent point-like dipoles, and eq 2 simplifies as $\gamma_t^{0D} \approx \gamma_0(z_0/d)^4$. Nevertheless, it must be emphasized that eq 2 applies to a point-like donor, while in our case, the NCs have a finite radius, larger than the thinnest MgO films (0.6 nm) deposited here. However, the surrounding ligands and the finite thickness of the CdS shell of our CdSe/CdS NCs warrant that there is a minimal distance of a few nanometers between the graphene layer and the emitting CdSe core. We will therefore consider that the *long distance* approximation is valid and neglect the finite size of the NCs and NPs. Considering random relative dipole orientation, we obtain[40] $z_0^4 = (3\alpha/2048\pi^3 F^2 \varepsilon^{5/2})\lambda_0^4$, where $\alpha \approx 1/137$ is the fine structure constant, ε is the effective dielectric constant (at λ_0) of the surrounding medium, and $F = 3\varepsilon/(\varepsilon_{CdS} + 2\varepsilon)$ is a screening factor.[59] Using $\varepsilon \approx (\varepsilon_{MgO} + 1)/2 \approx 2$ results in $z_0 \approx 12$ nm, in good agreement with our measurements.

We now address the distance dependence of the RET rate from single NPs to graphene. The NPs cores are atomically smooth and have recently been shown to behave as genuine quantum wells.[12] As a result, a different regime of RET is

DOI: 10.1021/nl5044192
Nano Lett. 2015, 15, 1252−1258

anticipated when a two-dimensional donor is involved. Electronic states in NPs are described by extended wave functions that are coherent over large distances in the NP plane. However, at finite temperature, one has to consider, in a photoexcited NP, a thermal distribution of excitons with different in-plane center of mass momentum. Besides, since the thickness of the NP shell is on the order of 2 nm, there is a minimal separation between the NP core and graphene, such that the approximation $d \gg 1/q_{max}$ holds (i.e., graphene can also be treated as an incoherent plane of point-like-dipoles). Similar situations have been previously modeled by Basko et al.[41] and Kos et al.[42] for hybrid systems composed of quantum wells transferring energy to an assembly (thick film or monolayer) of point-like dipoles. The calculated RET rate writes

$$\gamma_t^{2D}(d) \propto \int_0^\infty dq\, q^3 e^{-2qd} e^{-\left(\frac{\Lambda q}{2\pi}\right)^2} \quad (3)$$

where $\Lambda = h/(2m^*k_BT)^{1/2}$ is the de Broglie thermal length, with h the Planck constant, k_B the Boltzmann constant, and m^* the mass of the lowest energy heavy hole exciton ($m^* \approx m_e$, where m_e is the free electron mass) in CdSe.[12,60]

This expression applies to free excitons in an infinite quantum well, with thickness ($L_z \ll d$). The assumption of free excitons is consistent with the reported low density of trapping sites of CdSe-based core/shell NPs.[46] In addition, since the typical lateral dimensions of our NPs ($L_x = (22 \pm 2)$ nm and $L_y = (9 \pm 1.5)$ nm) exceed Λ (at room temperature, $\Lambda \approx 7.5$ nm), finite size effects can be neglected. We have thus attempted to fit the data in Figure 5b using the expression $\gamma(d) = \gamma_0 + \gamma_t^{2D}(d)$. A good agreement with our experimental results is obtained using $d_0 = (3.5 \pm 1)$ nm. Again, the latter value is consistent with the thickness of the core and shell of the NPs and includes a minor contribution from the surrounding ligands and residual adsorbates.

An analysis of the limiting cases of eq 3 provides a rationale for the observed scaling. In the short distance limit, $d \ll \Lambda$, γ_t^{2D} becomes independent of the distance and is determined by the thermal cutoff. In contrast, in the large distance (or high temperature) limit, $d \gg \Lambda$ and γ_t^{2D} follows a $1/d^4$ scaling, as expected in the case of a two-dimensional assembly of incoherent point-like dipoles. Since, at room temperature, Λ falls exactly in our measurement range, we expect the RET rate to decay more smoothly than $1/d^4$ for $d < \Lambda$. This is indeed observed experimentally (see Figure 5b), since a scaling based on eq 2, with $p = 4$ and $d_0 = 3.5$ nm, having asymptotic behavior for large d as our fit based on eq 3, would predict a higher γ in the short distance limit.

The results shown in Figure 5 suggest that, even at room temperature, the distance scaling of the RET rate from an extended donor (such as a two-dimensional NP) to graphene exhibits, as expected theoretically, a slight deviation from a simple power law. Following eq 3, this deviation should be more prominent at lower temperatures. Thus, further investigations of the distance and temperature dependence of the RET rate for various NP architectures could provide insights into the dimensionality of excitons in these novel systems.[36]

In conclusion, Förster-type resonant energy transfer dramatically affects the photophysics of semiconductor nanostructures absorbed on graphene. In spite of its atomic thinness, a single layer of graphene typically quenches more than 95% of the luminescence of individual nanocrystals or nanoplatelets. The observation of well-defined distance scalings of the resonant energy transfer rate suggests that novel graphene-based molecular rulers can be engineered using semiconductor nanostructures with different size, shape, and dimensionality. This is a promising development, especially for biological research. Finally, with the prospect of designing hybrid optoelectronic devices, we show that graphene can very efficiently harvest energy from photoexcited semiconductor nanostructures, which is of interest for photodetection. A major challenge is now to dissociate the electron−hole excitations generated in graphene before their fast relaxation into heat.[61,62]

■ ASSOCIATED CONTENT

Supporting Information

Synthesis and characterization of CdSe/CdS nanocrystals and CdSe/CdS/ZnS nanoplatelets, graphene growth by chemical vapor deposition, sample characterization by micro-Raman spectroscopy, definition of the energy transfer rate, and comparison of the normalized distance dependent decay rates. This material is available free of charge via the Internet at http://pubs.acs.org.

■ AUTHOR INFORMATION

Corresponding Author

*E-mail: stephane.berciaud@ipcms.unistra.fr.

Notes

The authors declare no competing financial interest.

■ ACKNOWLEDGMENTS

We are grateful to D. M. Basko and G. Weick for fruitful discussions, to R. Bernard, S. Siegwald, and H. Majjad for help with sample fabrication and characterization in the STNano clean room facility, and to M. Romeo for technical support. The authors at IPCMS acknowledge financial support from the CNRS, Université de Strasbourg, C'Nano GE, and the Agence Nationale de Recherche (ANR) under grants QuandDoGra ANR-12-JS10-0001 and Fungraph ANR-11-IS10-0003. B.D. (at ESPCI) thanks the ANR for funding under grants SNAP and QDOTICS. J.-O.L. (at KRICT) acknowledges support from NRF-ANR program through the National Rearch Foundation of Korea funded by the Ministry of Education, Science and Technology (NRF-2011-K2A1A5-2011-0031552).

■ REFERENCES

(1) Bonaccorso, F.; Sun, Z.; Hasan, T.; Ferrari, A. C. *Nat. Photonics* **2010**, *4*, 611−622.
(2) Koppens, F. H. L.; Mueller, T.; Avouris, P.; Ferrari, A. C.; Vitiello, M. S.; Polini, M. *Nat. Nanotechnol.* **2014**, *9*, 780−793.
(3) Talapin, D. V.; Lee, J.-S.; Kovalenko, M. V.; Shevchenko, E. V. *Chem. Rev.* **2010**, *110*, 389−458.
(4) Nair, R. R.; Blake, P.; Grigorenko, A. N.; Novoselov, K. S.; Booth, T. J.; Stauber, T.; Peres, N. M. R.; Geim, A. K. *Science* **2008**, *320*, 1308.
(5) Mak, K. F.; Sfeir, M. Y.; Wu, Y.; Lui, C. H.; Misewich, J. A.; Heinz, T. F. *Phys. Rev. Lett.* **2008**, *101*, 196405.
(6) Das Sarma, S.; Adam, S.; Hwang, E. H.; Rossi, E. *Rev. Mod. Phys.* **2011**, *83*, 407−470.
(7) Wang, X.; Zhi, L.; Müllen, K. *Nano Lett.* **2008**, *8*, 323.
(8) Kim, K. S.; Zhao, Y.; Jang, H.; Lee, S. Y.; Kim, J. M.; Kim, K. S.; Ahn, J.-H.; Kim, P.; Choi, J.-Y.; Hong, B. H. *Nature* **2009**, *457*, 706−710.
(9) Edited by Klimov, V. *Nanocrystal Quantum Dots*; CRC Press: UK, 2010.

DOI: 10.1021/nl5044192
Nano Lett. 2015, 15, 1252−1258

(10) Peng, X.; Manna, L.; Yang, W.; Wickham, J.; Scher, E.; Kadavanich, A.; Alivisatos, A. P. *Nature* **2000**, *404*, 59−61.
(11) Ithurria, S.; Dubertret, B. *J. Am. Chem. Soc.* **2008**, *130*, 16504−16505.
(12) Ithurria, S.; Tessier, M. D.; Mahler, B.; Lobo, R. P. S. M.; Dubertret, B.; Efros, A. L. *Nat. Mater.* **2011**, *10*, 936−941.
(13) Chen, Z.; Berciaud, S.; Nuckolls, C.; Heinz, T. F.; Brus, L. E. *ACS Nano* **2010**, *4*, 2964−2968.
(14) Ajayi, O. A.; Anderson, N. C.; Cotlet, M.; Petrone, N.; Gu, T.; Wolcott, A.; Gesuele, F.; Hone, J.; Owen, J. S.; Wong, C. W. *Appl. Phys. Lett.* **2014**, *104*, 171101.
(15) Rogez, B.; Yang, H.; Le Moal, E.; Lévêque-Fort, S.; Boer-Duchemin, E.; Yao, F.; Lee, Y.-H.; Zhang, Y.; Wegner, K. D.; Hildebrandt, N.; Mayne, A.; Dujardin, G. *J. Phys. Chem. C* **2014**, *118*, 18445−18452.
(16) Konstantatos, G.; Badioli, M.; Gaudreau, L.; Osmond, J.; Bernechea, M.; de Arquer, F. P. G.; Gatti, F.; Koppens, F. H. L. *Nat. Nanotechnol.* **2012**, *7*, 363.
(17) Sun, Z.; Liu, Z.; Li, J.; Tai, G.-a.; Lau, S.-P.; Yan, F. *Adv. Mater.* **2012**, *24*, 5878.
(18) Klekachev, A. V.; Asselberghs, I.; Kuznetsov, S. N.; Cantoro, M.; Mun, J. H.; Cho, B.-J.; Hotta, J.-i.; Hofkens, J.; van der Veen, M.; Stesmans, A. L.; Heyns, M. M.; De Gendt, S. *Proc. SPIE* **2012**, *8462*, 84620L.
(19) Klekachev, A. V.; Kuznetsov, S. N.; Asselberghs, I.; Cantoro, M.; Hun Mun, J.; Jin Cho, B.; Stesmans, A. L.; Heyns, M. M.; De Gendt, S. *Appl. Phys. Lett.* **2013**, *103*, 043124.
(20) Förster, T. *Ann. Phys.* **1948**, *437*, 55.
(21) Velizhanin, K. A.; Efimov, A. *Phys. Rev. B* **2011**, *84*, 085401.
(22) Gómez-Santos, G.; Stauber, T. *Phys. Rev. B* **2011**, *84*, 165438.
(23) Tielrooij, K. J. et al. *arXiv*: 1410.1361 **2014**.
(24) Lee, J.; Bao, W.; Ju, L.; Schuck, P. J.; Wang, F.; Weber-Bargioni, A. *Nano Lett.* **2014**, *14*, 7115−7119.
(25) Shafran, E.; Mangum, B. D.; Gerton, J. M. *Nano Lett.* **2010**, *10*, 4049−4054.
(26) Jander, S.; Kornowski, A.; Weller, H. *Nano Lett.* **2011**, *11*, 5179−5183.
(27) Lin, T. N.; Huang, L. T.; Shu, G. W.; Yuan, C. T.; Shen, J. L.; Lin, C. A. J.; Chang, W. H.; Chiu, C. H.; Lin, D. W.; Lin, C. C.; Kuo, H. C. *Opt. Lett.* **2013**, *38*, 2897−2899.
(28) Treossi, E.; Melucci, M.; Liscio, A.; Gazzano, M.; Samori, P.; Palermo, V. *J. Am. Chem. Soc.* **2009**, *131*, 15576−15577.
(29) Kim, J.; Cote, L. J.; Kim, F.; Huang, J. *J. Am. Chem. Soc.* **2009**, *132*, 260−267.
(30) Gaudreau, L.; Tielrooij, K. J.; Prawiroatmodjo, G. E. D. K.; Osmond, J.; de Abajo, F. J. G.; Koppens, F. H. L. *Nano Lett.* **2013**, *13*, 2030−2035.
(31) Stöhr, R. J.; Kolesov, R.; Xia, K.; Reuter, R.; Meijer, J.; Logvenov, G.; Wrachtrup, J. *ACS Nano* **2012**, *6*, 9175−9181.
(32) Tisler, J.; Oeckinghaus, T.; Stöhr, R. J.; Kolesov, R.; Reuter, R.; Reinhard, F.; Wrachtrup, J. *Nano Lett.* **2013**, *13*, 3152−3156.
(33) Wang, Y.; Li, Z.; Wang, J.; Li, J.; Lin, Y. *Trends Biotechnol.* **2011**, *29*, 205−212.
(34) Mazzamuto, G.; Tabani, A.; Pazzagli, S.; Rizvi, S.; Reserbat-Plantey, A.; Schädler, K.; Navickaite, G.; Gaudreau, L.; Cataliotti, F. S.; Koppens, F.; Toninelli, C. *New J. Phys.* **2014**, *16*, 113007.
(35) Halivni, S.; Sitt, A.; Hadar, I.; Banin, U. *ACS Nano* **2012**, *6*, 2758−2765.
(36) Rindermann, J. J.; Pozina, G.; Monemar, B.; Hultman, L.; Amano, H.; Lagoudakis, P. G. *Phys. Rev. Lett.* **2011**, *107*, 236805.
(37) Godel, F.; Pichonat, E.; Vignaud, D.; Majjad, H.; Metten, D.; Henry, Y.; Berciaud, S.; Dayen, J.-F.; Halley, D. *Nanotechnology* **2013**, *24*, 475708.
(38) Kuhn, H. *J. Chem. Phys.* **1970**, *53*, 101−108.
(39) Chance, R. R.; Prock, A.; Silbey, R. *Adv. Chem. Phys.* **1978**, *37*, 65.
(40) Swathi, R. S.; Sebastian, K. L. *J. Chem. Phys.* **2009**, *130*, 086101.
(41) Basko, D. M.; Agranovich, V. M.; Bassani, F.; Rocca, G. C. L. *Eur. Phys. J. B* **2000**, *13*, 653−659.
(42) Kos, S.; Achermann, M.; Klimov, V. I.; Smith, D. L. *Phys. Rev. B* **2005**, *71*, 205309.
(43) Mohamed, M. B.; Tonti, D.; Al-Salman, A.; Chemseddine, A.; Chergui, M. *J. Phys. Chem. B* **2005**, *109*, 10533−10537.
(44) Mahler, B.; Spinicelli, P.; Buil, S.; Quelin, X.; Hermier, J.-P.; Dubertret, B. *Nat. Mater.* **2008**, *7*, 659−664.
(45) Mahler, B.; Nadal, B.; Bouet, C.; Patriarche, G.; Dubertret, B. *J. Am. Chem. Soc.* **2012**, *134*, 18591−18598.
(46) Tessier, M. D.; Mahler, B.; Nadal, B.; Heuclin, H.; Pedetti, S.; Dubertret, B. *Nano Lett.* **2013**, *13*, 3321−3328.
(47) Hines, M. A.; Guyot-Sionnest, P. *J. Phys. Chem.* **1996**, *100*, 468−471.
(48) Li, X.; Cai, W.; An, J.; Kim, S.; Nah, J.; Yang, D.; Piner, R.; Velamakanni, A.; Jung, I.; Tutuc, E.; Banerjee, S. K.; Colombo, L.; Ruoff, R. S. *Science* **2009**, *324*, 1312−1314.
(49) Wang, W. H.; Han, W.; Pi, K.; McCreary, K. M.; Miao, F.; Bao, W.; Lau, C. N.; Kawakami, R. K. *Appl. Phys. Lett.* **2008**, *93*, 183107.
(50) Leatherdale, C. A.; Woo, W.-K.; Mikulec, F. V.; Bawendi, M. G. *J. Phys. Chem. B* **2002**, *106*, 7619−7622.
(51) Park, Y.-S.; Malko, A. V.; Vela, J.; Chen, Y.; Ghosh, Y.; Garcia-Santamaria, F.; Hollingsworth, J. A.; Klimov, V. I.; Htoon, H. *Phys. Rev. Lett.* **2011**, *106*, 187401.
(52) She, C.; Fedin, I.; Dolzhnikov, D. S.; Demortiére, A.; Schaller, R. D.; Pelton, M.; Talapin, D. V. *Nano Lett.* **2014**, *14*, 2772−2777.
(53) Cichos, F.; Vonborczyskowski, C.; Orrit, M. *Curr. Opin. Colloid Interface Sci.* **2007**, *12*, 272−284.
(54) Spinicelli, P.; Buil, S.; Quélin, X.; Mahler, B.; Dubertret, B.; Hermier, J.-P. *Phys. Rev. Lett.* **2009**, *102*, 136801.
(55) Malko, A. V.; Park, Y.-S.; Sampat, S.; Galland, C.; Vela, J.; Chen, Y.; Hollingsworth, J. A.; Klimov, V. I.; Htoon, H. *Nano Lett.* **2011**, *11*, 5213−5218.
(56) Tessier, M. D.; Javaux, C.; Maksimovic, I.; Loriette, V.; Dubertret, B. *ACS Nano* **2012**, *6*, 6751−6758.
(57) Swathi, R. S.; Sebastian, K. L. *J. Chem. Phys.* **2008**, *129*, 054703.
(58) Malic, E.; Appel, H.; Hofmann, O. T.; Rubio, A. *J. Phys. Chem. C* **2014**, *118*, 9283−9289.
(59) Califano, M.; Franceschetti, A.; Zunger, A. *Nano Lett.* **2005**, *5*, 2360−2364.
(60) Blachnik, R.; Chu, J.; Galazka, R.; Geurts, J.; Gutowski, J.; Hönerlage, B.; Hofmann, D.; Kossut, J.; Lévy, R.; Michler, P.; Neukirch, U.; Story, T.; Strauch, D.; Waag, A. In *Landolt-Börnstein, New Series III/41B*; Rössler, U., Ed.; Springer Verlag: Berlin, 1999.
(61) Johannsen, J. C.; Ulstrup, S.; Cilento, F.; Crepaldi, A.; Zacchigna, M.; Cacho, C.; Turcu, I. C. E.; Springate, E.; Fromm, F.; Raidel, C.; Seyller, T.; Parmigiani, F.; Grioni, M.; Hofmann, P. *Phys. Rev. Lett.* **2013**, *111*, 027403.
(62) Gierz, I.; Petersen, J. C.; Mitrano, M.; Cacho, C.; Turcu, I. C. E.; Springate, E.; Stöhr, A.; Köhler, A.; Starke, U.; Cavalleri, A. *Nat. Mater.* **2013**, *12*, 1119−1124.

DOI: 10.1021/nl5044192
Nano Lett. 2015, 15, 1252−1258